Metabolic Engineering 61 (2020) 152–159

Contents lists available at ScienceDirect

Metabolic Engineering

journal homepage: www.elsevier.com/locate/meteng

Construction of a carbon-conserving pathway for glycolate production by synergetic utilization of acetate and glucose in *Escherichia coli*

Yong Yu[a,b,c,1], Mengyao Shao[b,c,d,1], Di Li[b,c,d], Feiyu Fan[b,c], Hongtao Xu[b,c], Fuping Lu[d], Changhao Bi[b,c], Xinna Zhu[b,c,**], Xueli Zhang[b,c,*]

[a] University of Chinese Academy of Sciences, Beijing, 100049, China
[b] Tianjin Institute of Industrial Biotechnology, Chinese Academy of Sciences, Tianjin, 300308, China
[c] Key Laboratory of Systems Microbial Biotechnology, Chinese Academy of Sciences, Tianjin, 300308, China
[d] College of Biotechnology, Tianjin University of Sciences and Technology, Tianjin, 300457, China

ARTICLE INFO

Keywords:
Acetate
Glucose
Glycolate
Synergetic
Escherichia coli

ABSTRACT

Glycolate is a bulk chemical which has been widely used in textile, food processing, and pharmaceutical industries. Glycolate can be produced from sugars by microbial fermentation. However, when using glucose as the sole carbon source, the theoretical maximum carbon molar yield of glycolate is 0.67 mol/mol due to the loss of carbon as CO_2. In this study, a synergetic system for simultaneous utilization of acetate and glucose was designed to increase the carbon yield. The main function of glucose is to provide NADPH while acetate to provide the main carbon backbone for glycolate production. Theoretically, 1 glucose and 5 acetate can produce 6 glycolate, and the carbon molar yield can be increased to 0.75 mol/mol. The whole synthetic pathway was divided into two modules, one for converting acetate to glycolate and another to utilize glucose to provide NADPH. After engineering module I through activation of *acs*, *gltA*, *aceA* and *ycdW*, glycolate titer increased from 0.07 to 2.16 g/L while glycolate yields increased from 0.04 to 0.35 mol/mol-acetate and from 0.03 to 1.04 mol/mol-glucose. Module II was then engineered to increase NADPH supply. Through deletion of *pfkA*, *pfkB*, *ptsI* and *sthA* genes as well as upregulating *zwf*, *pgl* and *tktA*, glycolate titer increased from 2.16 to 4.86 g/L while glycolate yields increased from 0.35 to 0.82 mol/mol-acetate and from 1.04 to 6.03 mol/mol-glucose. The activities of AceA and YcdW were further increased to pull the carbon flux to glycolate, which increased glycolate yield from 0.82 to 0.92 mol/mol-acetate. Fed-batch fermentation of the final strain NZ-Gly303 produced 73.3 g/L glycolate with a productivity of 1.04 g/(L·h). The acetate to glycolate yield was 0.85 mol/mol (1.08 g/g), while glucose to glycolate yield was 6.1 mol/mol (2.58 g/g). The total carbon molar yield was 0.60 mol/mol, which reached 80% of the theoretical value.

1. Introduction

Glycolic acid ($HOCH_2COOH$) is the simplest α-hydroxy acid, which has the dual properties of acid and alcohol, and is widely used in textile, food processing, and pharmaceutical industries (Zahoor et al., 2014; Deng et al., 2018). Moreover, glycolate is extensively used in the manufacturing of cleaning agent formulations as well as skin care creams and shampoos. The demand for glycolate has increased significantly in recent years and its global market is expected to be 415 million US dollars by 2024 (Deng et al., 2018). At present, glycolate is manufactured through the chemical carbonylation of formaldehyde (Loder, 1939) or by nitrilase catalyzing hydrolysis of glycolonitrile (He et al., 2010). However, these processes involve harsh conditions or toxic by-products. Microorganisms such as *Pichia naganishii* (Kataoka et al., 2001) and *Gluconobacter oxydans* (Wei et al., 2009) can oxidize ethylene glycol to glycolate, yet the cost is too expensive.

To produce glycolate by the economically feasible and environmental friendly ways, many efforts have been made by metabolic engineering of microorganisms, especially by engineered *Escherichia coli* using glucose as sole carbon source. Glycolate can be synthesized from glyoxylate by glyoxylate reductase, while glyoxylate can be generated through glycolysis and glyoxylate bypass pathway (Fig. 1). Through over-expressing isocitrate lyase and glyoxylate reductase, as well as decreasing the expression of isocitrate dehydrogenase, an engineered *E.*

* Corresponding author. 32 West 7th Ave, Tianjin Airport Economic Park, Tianjin, 300308, China.
** Corresponding author. 32 West 7th Ave, Tianjin Airport Economic Park, Tianjin, 300308, China.
E-mail addresses: zhu_xn@tib.cas.cn (X. Zhu), zhang_xl@tib.cas.cn (X. Zhang).
[1] These authors contributed equally to this work.

https://doi.org/10.1016/j.ymben.2020.06.001
Received 16 February 2020; Received in revised form 5 May 2020; Accepted 1 June 2020
Available online 10 June 2020

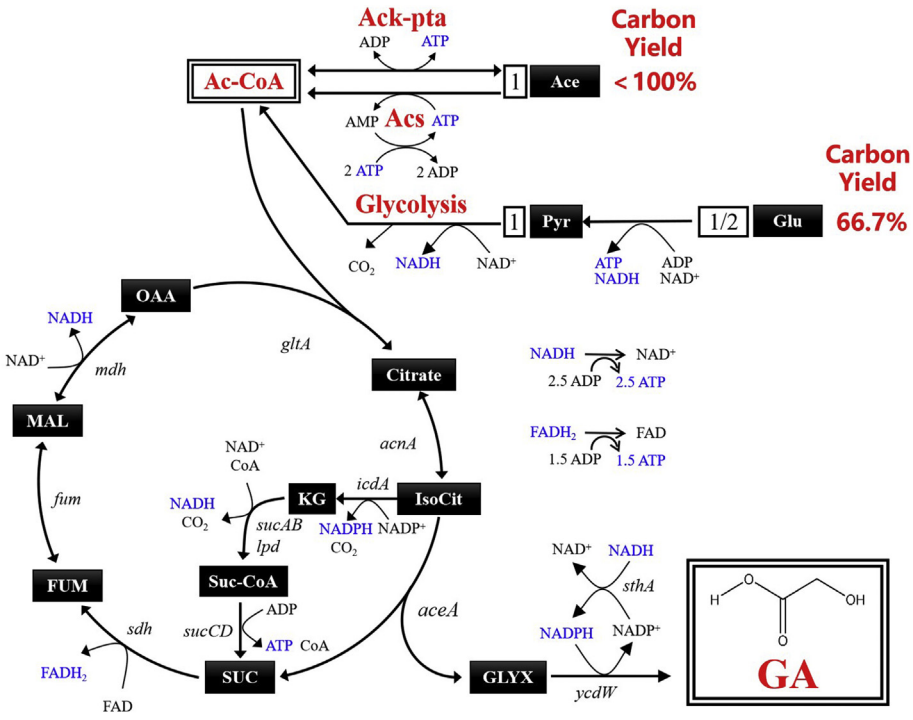

Fig. 1. Metabolic pathways for the produce of glycolate using acetate or glucose as the sole carbon source. NADH and $FADH_2$ can be converted to 2.5 mol of and 1.5 mol of ATP (Hinkle, 1981). The boxed numbers between some metabolites represent stoichiometry. Abbreviations: Glu, glucose; Ace, acetate; Ac-CoA, acetyl-CoA; OAA, oxaloacetate; IsoCit, isocitrate; GLYX, glyoxylate; GA; glycolate; KG, α-ketoglutarate; Suc-CoA, succinyl-CoA; SUC, succinate; FUM, fumarate; MAL, malate; *gltA*, citrate synthase; *acnA*, aconitate hydratase A; *aceA*, isocitrate lyase; *icdA*, isocitrate dehydrogenase; *sucAB*, 2-oxoglutarate decarboxylase and dihydrolipoyltranssuccinylase; *lpd*, lipoamide dehydrogenase; *sucCD*, succinyl-CoA synthetase subunit α and β; *sdh*, succinate dehydrogenase; *fum*, fumarase; *mdh*, malate dehydrogenase; *ycdW*, glyoxylate reductase; *sthA*, soluble pyridine nucleotide transhydrogenase; *ack*, acetate kinase; *pta*, phosphate acetyltransferase; *acs*, acetyl-CoA synthetase.

coli strain AG0956 produced 52.2 g/L glycolate with molar yield of 0.9 mol/mol-glucose and productivity of 1.33 g/(L·h) (Dischert and Soucaille, 2015). Through activating the expressions of isocitrate lyase, isocitrate dehydrogenase kinase/phosphatase, glyoxylate reductase and citrate synthase, an engineered *E. coli* strain Mgly434 produced 65.5 g/L glycolate with molar yield of 1.81 mol/mol-glucose and productivity of 0.85 g/(L·h) (Deng et al., 2018). The theoretical molar yield of glycolate from glucose is 2 mol/mol (Koivistoinen et al., 2013), yet the carbon molar yield is only 0.67 mol/mol due to the carbon loss during the conversion of pyruvate to acetyl-CoA (Fig. 1).

In contrast to glucose, acetate can be converted to acetyl-CoA by acetyl-CoA synthetase (Acs) or acetate kinase-phosphotransacetylase (Ack-pta), and no carbon is lost. However, all the carbon can not be converted to glycolate when using acetate as the sole carbon source. Carbon needs to be consumed to generate ATP and reducing equivalent to support acetate assimilation and glycolate production (Fig. 1). When converting acetate to acetyl-CoA, Ack-pta pathway requires 1 mol of ATP, while Acs requires 2 mol of ATP (Xiao et al., 2013). On the other hand, reducing equivalent is required for converting acetyl-CoA to glycolate, while no reducing equivalent is generated during the conversion of acetate to acetyl-CoA. Thus, acetyl-CoA needs to go through the oxidative TCA cycle to generate reducing equivalent, but at the cost of carbon loss as CO_2, which would lead to low product yield (Fig. 1).

In this study, a synergetic system for simultaneous utilization of acetate and glucose to produce glycolate was designed to increase the carbon yield. The main function of glucose is to provide reducing equivalent while acetate to provide the main carbon backbone for glycolate production. High carbon molar yield was obtained using this synergetic system.

2. Materials and methods

2.1. Strains, media and growth conditions

Strains used in this study are listed in Table 1. During strain construction, cultures were grown aerobically at 30 °C, 37 °C in Luria broth (per liter: 10 g Difco tryptone, 5 g Difco yeast extract and 10 g NaCl). For preparing solid medium, 15 g/L agar powder was added to Luria broth. Ampicillin (100 mg/L), kanamycin (50 mg/L), or chloramphenicol (34 mg/L) were used where appropriate. L-(+)-arabinose (10 g/L) is used to induce CRISPR/Cas9 system and Red homologous recombination system during gene deletion and integration.

2.2. Gene deletion and integration

All *E. coli* gene knockouts and gene insertions were performed using two-plasmid CRISPR/Cas9 technology as reported previously (Zhao et al., 2016; Zhu et al., 2017). The donor plasmids (Table S1) were optimized and the details of two-plasmid CRISPR/Cas9 technology were described in Text S1. The primers used for gene deletions, integration and modulations are listed in Table S2.

2.3. Modulation of gene expression with RBS library or T7 promoter

A two-step homologous recombination method was used to modulate *aceA*, *gltA*, *zwf*, *pgl* and *tktA* genes with an RBS library (RBSL) as described previously (Chen et al., 2014; Tan et al., 2016). Taking construction of aceA-RBSL for instance, the aceA-cat-sacB DNA fragment was amplified from pXZ-CS plasmid (Tan et al., 2013) with primer set aceA-cat-sacB-up/down and inserted before the ATG start codon of the *aceA* gene. Then, primer set aceA-P-up/aceA-RBSL-down was used to PCR amplify the aceA-RBSL DNA fragment for the second recombination step, using the genomic DNA of *E. coli* strain M1-93 (Lu et al., 2012) as the template. After PCR verification using primer set aceA-YZ-up/down, twelve colonies were randomly picked for AceA enzyme activity assays. The strain with the highest activity was selected for the next round genetic modification.

The native promoters of *acs* and *ycdW* genes were replaced by T7 promoter using the same two-step homologous recombination method (Chen et al., 2014; Tan et al., 2016). For the second recombination, DNA fragment containing T7 promoter was amplified from pUC57-T7 (synthesized by Genscript, China) using primer sets acs-TK-up-T7/acs-TK-down-T7 or ycdW-TKup-T7/ycdW-TK-down-T7 (Table S2). The right colonies verified by PCR were selected for further enzyme activity assays and fermentations.

Table 1
Strains used in this study.

Name	Characteristics	Source or reference
ATCC 8739	Wild type	Lab collection
BL21-DE3	F^-, *ompT*, *hsdS* (rBB-mB-), *gal*, *dcm* (DE3)	Lab collection
NZ-Gly012	ATCC 8739, Δ*aceB*, Δ*gcl*, Δ*ldhA*, Δ*glcDEF*, Δ*aldA*	This work
T7-YcdW	NZ-Gly012, T7-*ycdW*, Δ*rhaBAD*-T7-RNAP	This work
T7-AckA	NZ-Gly012, T7-*ycdW*, T7-*ackA*, Δ*rhaBAD*-T7-RNAP	This work
T7-Acs	NZ-Gly012, T7-*ycdW*, T7-*acs*, Δ*rhaBAD*-T7-RNAP	This work
R-GltA	NZ-Gly012, T7-*ycdW*, T7-*acs*, RBSL1-*gltA*, Δ*rhaBAD*-T7-RNAP	This work
NZ-Gly034 (R-AceA)	NZ-Gly012, T7-*ycdW*, T7-*acs*, RBLS1-*gltA*, Δ*iclR*, RBSL12-*aceA*, Δ*rhaBAD*-T7-RNAP	This work
D-Pfk	NZ-Gly034, Δ*pfkA*, Δ*pfkB*, Δ*ptsI*	This work
R-Zwf	NZ-Gly034, Δ*pfkA*, Δ*pfkB*, Δ*ptsI*, RBSL9-*zwf*	This work
R-Pgl	NZ-Gly034, Δ*pfkA*, Δ*pfkB*, Δ*ptsI*, RBSL9-*zwf*, RBSL8-*pgl*	This work
R-TktA	NZ-Gly034, Δ*pfkA*, Δ*pfkB*, Δ*ptsI*, RBSL9-*zwf*, RBSL8-*pgl*, RBSL3-*tktA*	This work
NZ-Gly066 (D-SthA)	NZ-Gly034, Δ*pfkA*, Δ*pfkB*, Δ*ptsI*, RBSL9-*zwf*, RBSL8-*pgl*, RBSL3-*tktA*, Δ*sthA*	This work
D-IdA	NZ-Gly066, Δ*icdA*	This work
Tw-YcdW	NZ-Gly066, Δ*araBAD*-T7-*ycdW*	
NZ-Gly303 (Tw-AceA)	NZ-Gly066, Δ*araBAD*-T7-*ycdW*, Δ*mgsA*-PrrnD-*aceA*	This work

2.4. Enzyme activity assays

The activities of YcdW, AceA, GltA, Acs, Zwf, Pgl and TktA were determined as described previously (Zahoor et al., 2014; Honer Zu Bentrup et al., 1999; Underwood et al., 2002; Castano-Cerezo et al., 2009; Kabir and Shimizu, 2003; Stanford et al., 2004; Sobota et and Imlay, 2011).

Crude extracts were prepared from cells harvested during the mid-log phase (24 h) of fermentation. Collected cells were first washed with 50 mM Tris buffer (pH 7.0) twice, then suspended in the same buffer with 1 × protease inhibitor (Roche, Switzerland) to an OD_{550nm} of 10 for sonication treatment. After centrifugation at 12,000 × *g* and 4 °C for 20 min, the supernatant was transferred to a new tube. Bio-Rad Protein Assay Kit (Bio-Rad, USA) was used to measure protein concentration of the crude extract. One unit (U) of enzyme activity represents the amount of enzyme catalyzing the conversion of 1 μmol of substrate per min into specific product (1U/mg = μmol/min/mg protein). The details for enzyme activity assays are described in Text S1.

2.5. Fermentation

For analyzing glycolate production in shake flasks, single colonies were picked from the plate and inoculated into 15 mm × 100 mm tubes containing 2 mL LB and grown at 37 °C and 250 rpm overnight. Seed culture was then inoculated into 100 mL flasks containing 20 mL NBS mineral salts medium (Chen et al., 2014) with 5 g/L glucose, 10 g/L sodium acetate and an initial OD_{550nm} of 0.1. For strains using Ptrc promoter for induction of T7 RNAP gene, IPTG (1 mM) was added. After 24 h growth at 37 °C and 250 rpm, cells were collected for measurement of glycolate production.

Strain NZ-G303 was used for production of glycolate through fed-batch fermentation. Seed cultivation was prepared by inoculating 1 mL pre-culture into 500 mL shake flasks containing 100 mL Luria-Bertani (LB) medium, and incubated at 37 °C and 250 rpm for 12 h. The seed was then transferred to a 5 L bioreactor (Labfors 4; infors biotechnology Co. Ltd.) containing 3 L AM1 mineral salts medium (Zhu et al., 2014) with 28 g/L glucose, 5.2 g/L sodium acetate (equal to 3.8 g/L acetate), and 2 g/L yeast extract. The initial OD_{550nm} was 0.1, and IPTG (0.1 mM) was added when cells grown to OD_{550nm} of 0.5. Fermentation was carried out at 37 °C with an air flow rate of 3 L/min. The dissolved oxygen was kept at 25% by adjusting the agitation speed from 200 to 500 rpm. The pH was controlled at 7.0 by automatic addition of acetic acid. The fed solutions were 615 g/L sodium acetate and 800 g/L glucose respectively. During the feeding, the concentrations of glucose and acetate in fermentor were contained less than 10 and 5 g/L, respectively.

2.6. Analytical procedures

Cell growth was assayed by measuring the optical density at 550 nm (OD_{550nm}) using a SP-723 spectrophotometer (Spectrum SHANGHAI, China). The concentrations of acetate, glucose and glycolate were measured using high-performance liquid chromatography (Aminex HPX-87H, 7.8 × 300 mm, Bio-Rad) with a refractive index detector (RI-150 Thermo Spectra, USA). A mobile phase of 5 mM H_2SO_4 at a 0.5 mL/min flow rate was used at 35 °C.

3. Results and discussion

3.1. System design for synthetic utilization of acetate and glucose

For biosynthesis chemical product, the carbon yield, indicating carbon loss in the pathway, has a major impact on the overall economy of biorefinery and the carbon efficiency of cell growth (Bogorad et al., 2013). Glycolate can be produced from sugar in the engineered *E. coli*. However, when using glucose as the sole carbon source, the theoretical maximum carbon molar yield of glycolate is only 0.67 mol/mol, implying carbon loss during the process of glucose to acetyl-CoA. In contrast to glucose, acetate can be converted to acetyl-CoA with no carbon loss. More than that, the carbon content of acetic acid and glucose is equivalent, they both contain 1 carbon atom per 30 molecular weight, and the prices of acetate and glucose are about $324 and $479 per ton respectively. Thus, the mass of acetate is 32% more than that of glucose under the same price. However, all the carbon cannot be converted to glycolate when using acetate as the sole carbon source. Carbon needs to be consumed to generate ATP and reducing equivalent to support acetate assimilation, glycolate production and cell growth.

Here, a system was designed for synergetic utilization of acetate and glucose to increase carbon yield. In this system, the main function of glucose is to provide NADPH so that all the carbon of acetate can be reserved and converted to target products (Fig. 2). There are three strategies to generate NADPH by glucose catabolism through pentose phosphate pathway (Kim et al., 2011; Siedler et al., 2013; Wang et al., 2013). The first one is inactivation of phosphoglucose isomerase (Pgi) (Kim et al., 2011). Pgi is the second enzyme of the glycolysis pathway that converts glucose-6-phosphate to fructose-6-phosphate. Inactivation of Pgi pushes glucose carbon flux exclusively into the pentose phosphate pathway. Two mol of NADPH are produced from 1 mol of glucose by two redox reactions (glucose-6-phosphate dehydrogenase and 6-phosphogluconate dehydrogenase). The second strategy is inactivation of phosphofructokinase (Pfk) (Wang et al., 2013). Pfk catalyzes phosphorylation of fructose-6-phosphate to fructose-1,6-biphosphate. If Pfk is inactivated, fructose 6-phosphate has to reenter the pentose phosphate pathway to generate NADPH. In this situation, 1 mol of glucose

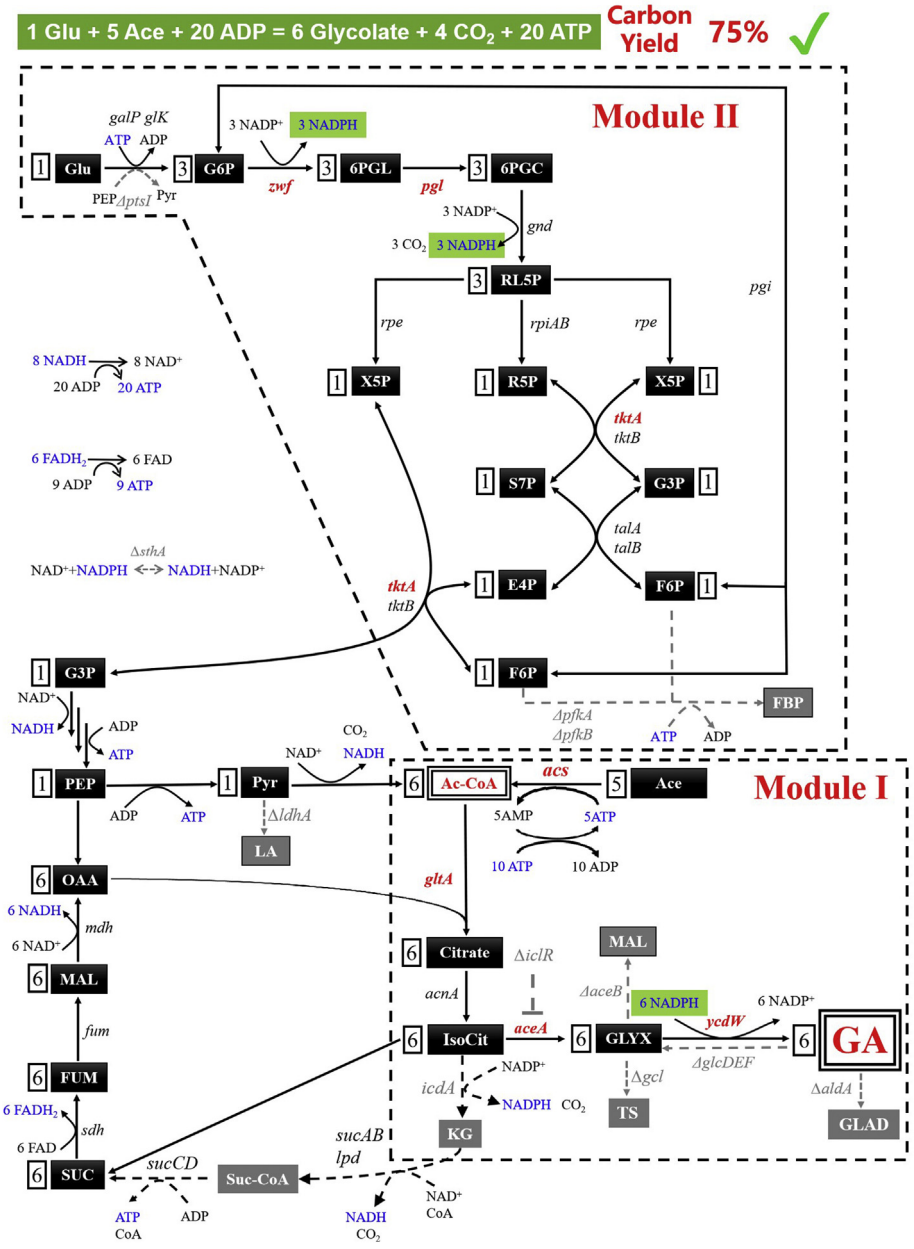

Fig. 2. Metabolic pathways for production of glycolate from acetate and glucose.

can be converted to 6 mol of NADPH, 1 mol of glyceraldehyde-3-phosphate and 3 mol of CO_2 (Fig. 2). The third strategy is inactivation of glyceraldehyde-3-phosphate dehydrogenase (GADPH) (Sielder et al., 2013), which would block conversion of glyceraldehyde-3-phosphate to 1,3-bisphospho-glycerate for downstream glycolysis. Glyceraldehyde-3-phophate goes back into the pentose phosphate pathway, leading a complete oxidation of glucose and generating 12 mol of NADPH from 1 mol of glucose. Although this strategy generates the most NADPH, *E. coli* cells cannot grow due to shortage of several essential building blocks, such as glycerate-3-phosphate, phosphoenolpyruvate (PEP) and C4 compounds (Lin et al., 2018). Thus, the second strategy was selected in this study to generate 6 mol of NADPH from 1 mol of glucose. It should be noted that glucose usually enters the *E. coli* cell through the PEP: sugar phosphotransferase system (PTS). The PTS system should be inactivated, otherwise half of glucose will be converted to PEP and cannot generate NADPH. When using the second strategy, 1 mol of glucose and 5 mol of acetate can be co-utilized to produce 6 mol of glycolate (Fig. 2). One mol of NADH and $FADH_2$ can be converted to 2.5 and 1.5 mol of ATP (Hinkle, 1981), so the whole pathway generates 20 mol of ATP, which would guarantee the energy supply (Fig. 2). The carbon molar yield is 75%, which is better than using glucose as the sole carbon source (66.7%).

3.2. Engineering module I for improving glycolate production

The whole synthetic pathway for producing glycolate from acetate and glucose is divided into two modules. Module I function is to synthesize glycolate from acetate. Module II is used to provide NADPH using glucose as the auxiliary carbon source. These two modules were engineered to improve glycolate production.

First, competing pathways consuming glycolate and its direct precursor glyoxylate were inactivated by deletion. Malate synthase (AceB), which catalyzes the condensation of glyoxylate and acetyl-CoA to form malate, and glyoxylate carboligase (Gcl), which catalyzes the condensation of two glyoxylate molecules to form tartronate semialdehyde, were inactivated. It should be noted that the native promoter of *aceB*

Table 2
Production of glycolate by the representative engineered *E. coli* strains.

Strain[a]	Glycolate titer (g/L)	Glycolate Yield (mol/mol-acetate)	Glycolate Yield (mol/mol-glucose)	Acetate consumption rate (g/gDCW·h)	Dry Cell Weight (g/L)
Wild-type	0	0	0	0	2.32 ± 0.01
NZ-Gly012	0.07 ± 0.00	0.04 ± 0.00	0.03 ± 0.00	0.03 ± 0.00	2.03 ± 0.01
NZ-Gly034	2.16 ± 0.02	0.35 ± 0.02	1.04 ± 0.11	0.14 ± 0.00	1.42 ± 0.01
NZ-Gly066	4.86 ± 0.15	0.82 ± 0.01	6.02 ± 0.12	0.18 ± 0.01	1.09 ± 0.01
NZ-Gly303	7.20 ± 0.22	0.92 ± 0.03	5.42 ± 0.13	0.25 ± 0.00	1.02 ± 0.00

[a] Fermentations were performed in shake flasks. Three repeats were performed and the error bars represent standard deviation.

gene was left in the chromosome since it is the promoter for the *aceBAK* gene operon. Glycolate dehydrogenase (GlcDEF), which catalyzes oxidation of glycolate to glyoxylate, and aldehyde dehydrogenase (AldA), which catalyzes conversion of glycolate to glycolaldehyde, were also inactivated. In addition, lactate dehydrogenase (LdhA), which converts pyruvate to D-lactate, was inactivated so that pyruvate produced from glucose can all go to acetyl-CoA for glycolate production. After deleting *aceB*, *gcl*, *glcDEF*, *aldA* and *ldhA* genes in *E. coli* ATCC 8739, an initial strain NZ-Gly012 was obtained. In shake flask fermentation, strain NZ-Gly012 produced 0.07 g/L glycolate in 24 h using acetate and glucose as double carbon sources while the wild type strain ATCC 8739 had no glycolate production (Table 2).

Next, module I was engineered to increase acetate assimilation rate and glycolate productivity. Module I consists of five enzymes, including acetyl-CoA synthetase (Acs), citrate synthase (GltA), aconitase (Acn), isocitrate lyase (AceA) and glyoxylate reductase (YcdW). The activities of these five enzymes of strain NZ-Gly012 were measured. Among them, Acs, GltA, AceA and YcdW had relatively low activities, ranging from 0.06 to 0.14 U/mg protein (Table 3). It was hypothesized that the low activities of these four enzymes limited acetate assimilation and glycolate production, and should be enhanced. Promoter engineering has been commonly used to increase the transcriptional levels of target genes and the related enzyme activities. In this study, either T7 or other artificial promoters were used to replace the native promoters of these four genes to increase the activity of module I. To support the expression of T7 promoter, the T7 RNA polymerase (RNAP) gene (Temme et al., 2012) of *E. coli* strain BL21-DE3 was integrated in the *rhaBAD* site of strain NZ-Gly012 and expressed under the control of *trc* promoter.

Glyoxylate reductase is the last enzyme of module I, which reduces glyoxylate to glycolate, coupled with NADPH oxidation to $NADP^+$. T7 promoter was used to replace the native promoter of *ycdW* gene using a two-step markerless modulation method (Zhao et al., 2013), resulting in strain T7-YcdW. As expected, the activity of YcdW increased significantly to 1.94 U/mg protein, which was 24-fold higher than that of the parent strain NZ-Gly012 (Table 3). Strain T7-YcdW produced 0.65 g/L glycolate, which was 8-fold higher than that of strain NZ-Gly012 (Fig. 3A). The glycolate yields were 0.23 mol/mol-acetate and 0.32 mol/mol-glucose, respectively (Fig. 3B).

Table 3
Improvement of key enzyme activities in the engineered *E. coli* strains after activation.

Enzymes	Enzyme activities (μmol/min/mg protein)[a]		Relative activity
	Before activation	After activation	
YcdW (EC1.1.1.79)	0.08 ± 0.02	1.94 ± 0.20	24.0
Acs (EC 6.2.1.1)	0.06 ± 0.01	0.52 ± 0.01	8.7
GltA (EC 2.3.3.1)	0.08 ± 0.01	0.48 ± 0.02	6
AceA (EC 4.1.3.1)	0.14 ± 0.01	1.68 ± 0.10[b]	12
Zwf (EC1.1.1.49)	0.13 ± 0.01	1.80 ± 0.10	13.8
Pgl (EC 3.1.1.31)	0.71 ± 0.06	1.60 ± 0.05	2.3
TktA (EC 2.2.1.1)	0.07 ± 0.02	0.96 ± 0.03	13.7

[a] Three repeats were performed and the error bars represent standard deviation.
[b] Isocitrate lyase activity after deletion of the *iclR* gene and modulation with an artificial promoter.

Next we sought to activate the acetate assimilation pathway to achieve a higher acetate consumption rate. Both the Ack-pta and Acs pathways were activated by replacing the native promoters with T7 promoter. The resulting strains T7-AckA and T7-Acs showed no significant difference in growth (Fig. S1C). Although acetate consumption rate of strain T7-AckA increased 2.6-fold compared to the parent strain T7-YcdW, glycolate titer had nearly no improvement (Figs. S1A and B). Strain T7-Acs produced 1.4 g/L glycolate and with an acetate consumption rate of 0.11 g/(gDCW·h), both of which were 2.2-fold higher than the parent strain (Fig. 3A; Figs. S1A and B). The glycolate yields of strain T7-Acs were 0.23 mol/mol-acetate and 0.68 mol/mol-glucose, respectively (Fig. 3B). Although Acs pathway requires 2 mol of ATP for converting acetate to acetyl-CoA while Ack-pta pathway requires only 1 mol of ATP, it was suggested that Acs was better than Ack-pta pathway for acetate assimilation. Calculated from the eQuillibrator database (pH 7.0, ionic strength 0.1 mol/L), the ΔG of Ack-pta pathway is 23.2 kJ/mol, whereas that of Acs pathway is -4.5 kJ/mol (Flamholz et al., 2012). The Acs pathway is more thermodynamically favorable, which might explain the beneficial effect on acetate assimilation.

Citrate synthase is a key enzyme of the TCA cycle and has been regarded as a rate-limiting enzyme when using acetate as the carbon source (Walsh and Koshland, 1985). It was thought that enhancing the activity of citrate synthase should increase the flux from oxaloacetate (OAA) and acetyl-CoA to citrate, and thus boost acetate assimilation. The native promoter of the *gltA* gene of strain T7-Acs was replaced by an RBS library (Tan et al., 2016), and twelve strains verified by PCR were picked for enzyme activity assays. The highest citrate synthase activity was 0.48 U/mg protein, which was 6-fold higher than the parent strain T7-Acs (Table 3). The resulting strain, designated as R-GltA, produced 1.52 g/L glycolate which was 9% higher than the parent strain T7-Acs (Fig. 3A). The glycolate yields of strain R-GltA were almost the same as the parent strain T7-Acs (Fig. 3B).

Isocitrate lyase, which converts isocitrate to glyoxylate and succinate, was the last one of module I to be engineered. Since the transcriptional regulator IclR represses the expression of the *aceBAK* gene operon (Zheng et al., 2010), the *iclR* gene was deleted, leading to a significant increase of isocitrate lyase activity from 0.14 to 0.45 U/mg protein, which was similar to previous reports (Noh et al., 2018; Holms et al., 1971). The expression level of *aceA* gene was further improved by modulation with an RBS library (Tan et al., 2016). Twelve strains verified by PCR were picked for enzyme activity assays. The highest isocitrate lyase activity was 1.68 U/mg protein, which was 12-fold higher than the parent strain R-GltA (Table 3). This strain, designated as R-AceA, produced 2.16 g/L glycolate which was 42% higher than the parent strain R-GltA (Fig. 3A). The glycolate yields of strain R-AceA were 0.35 mol/mol-acetate and 1.04 mol/mol-glucose, which were 46% and 44% higher than the parent strain R-GltA, respectively (Fig. 3B). Strain R-AceA was re-named as NZ-Gly034 (Table 1).

After engineering module I through activating acetyl-CoA synthetase, citrate synthase, isocitrate lyase and glyoxylate reductase, glycolate titer increased from 0.07 to 2.16 g/L while glycolate yields increased from 0.04 to 0.35 mol/mol-acetate and from 0.03 to 1.04 mol/mol-glucose (Table 2; Fig. 4).

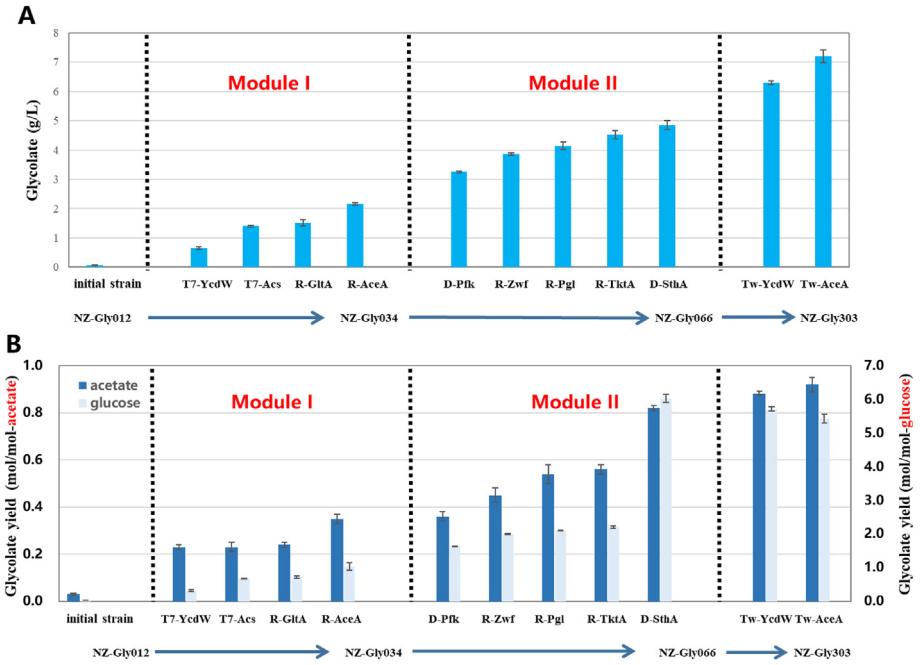

Fig. 3. Glycolate titer (A) and yields (B) of representative engineered *E. coli* strains. Fermentations were performed in shake flasks. Three repeats were performed and the error bars represent standard deviation.

3.3. Engineering module II for improving NADPH supply

Although glycolate titer increased significantly after activating module I, glycolate yield, especially glucose to glycolate yield, was still at a relatively low level (1.04 mol/mol). It was suggested that NADPH produced through module II was deficient for glycolate production. Thus, module II was engineered to improve NADPH supply.

First, two phosphofructokinase encoding genes (*pfkA* and *pfkB*) and *ptsI* gene of strain NZ-Gly034 were deleted, resulting in strain D-Pfk. This strain produced 3.25 g/L glycolate, which was 50% higher than the parent strain (Fig. 3A). Glucose to glycolate yield increased from 1.04 to 1.64 mol/mol (Fig. 3B), but still much lower than the designed theoretical maximum. It was thought that activity of the pentose phosphate pathway might not be high enough to support the NADPH supply.

Glucose-6-phosphate dehydrogenase (Zwf), 6-phosphogluconolactonase (Pgl) and transketolase (Tkt) are three key enzymes of the pentose phosphate pathway, and activation of them has been demonstrated to increase carbon flux through the pentose phosphate pathway, leading to increased supply of reducing equivalent and succinate production (Tan et al., 2016). Activities of these three enzymes were determined, ranging from 0.07 to 0.71 U/mg protein (Table 3). RBS libraries were used to replace the native promoters of *zwf*, *pgl* and *tktA* genes to increase their activities. After modulating *zwf* gene, twelve strains verified by PCR were picked for enzyme activity assays and the strain having the highest activity was picked for further modulation of *pgl* gene, then *tktA* gene. Activities of Zwf, Pgl and TktA in the resulting strain R-TktA were 1.8, 1.6 and 0.96 U/mg protein, which were 13.8-, 2.3- and 13.7-fold higher than the parent strain D-Pfk (Table 3). Strain R-TktA produced 4.52 g/L glycolate which was 40% higher than the parent strain D-Pfk (Fig. 3A). The glucose to glycolate yield increased from 1.64 to 2.2 mol/mol, while the acetate to glycolate yield increased from 0.36 to 0.56 mol/mol (Fig. 3B). Although activating pentose phosphate pathway increased the glucose to glycolate yield by 34%, it was still much lower than the designed theoretical maximum.

In *E. coli*, SthA is a soluble transhydrogenase responsible for

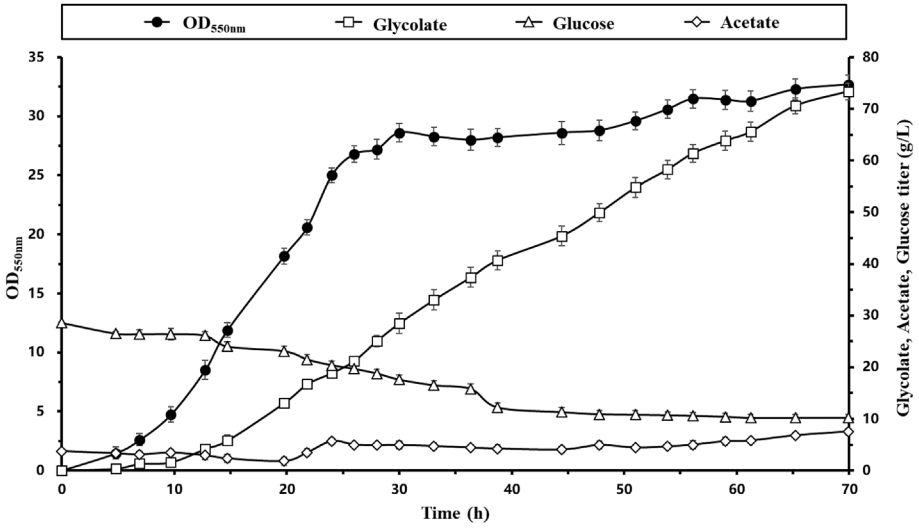

Fig. 4. Fed-batch fermentation profile of strain NZ-Gly303. The initial fermentation medium contained 3.8 g/L acetate and 28 g/L glucose. The pH was controlled at 7.0. During the feeding, the concentrations of glucose and acetate in fermentor were contained less than 10 and 5 g/L, respectively. The data points represent averages and standard deviations of three replicates.

converting NADPH into NADH (Sauer et al., 2004). It was thought that NADPH generated through pentose phosphate pathway might be consumed by SthA, thus decreasing the glucose to glycolate yield. Thus, *sthA* gene was deleted in strain R-TktA, resulting in strain NZ-Gly066 (also named D-SthA). The glucose to glycolate yield increased 2.7-fold to 6.03 mol/mol after deletion of *sthA* gene (Fig. 3B). The acetate to glycolate yield also increased from 0.56 to 0.82 mol/mol (Fig. 3B). This result suggested that eliminating the interconversion between NADPH and NADH was essential to provide a high NADPH supply.

After engineering module II through deletion of *pfkA*, *pfkB*, *ptsI* and *sthA* genes as well as activating Zwf, Pgl and TktA, glycolate titer increased from 2.16 to 4.86 g/L while glycolate yields increased from 0.35 to 0.82 mol/mol-acetate and from 1.04 to 6.03 mol/mol-glucose (Table 2).

3.4. Re-engineering module I for further improving glycolate production

Although acetate to glycolate yield increased from 0.04 to 0.82 mol/mol after engineering Module I and Module II, it was still lower than the designed theoretical maximum (1.2 mol/mol-acetate). It was thought that isocitrate was an important node (Zhu et al., 2019). If isocitrate is converted to α-ketoglutarate through isocitrate dehydrogenase (encoded by *icdA* gene) and the carbon flux goes into the TCA cycle, less carbon flux would go to glycolate. Therefore, the *icdA* gene was deleted in strain NZ-Gly066 to block the TCA cycle. However, the resulting strain D-IcdA did not grow on minimal salts medium. With the addition of α-ketoglutarate or succinate, cell growth was improved but glycolate production decreased significantly (data not shown).

Since it was difficult to block the TCA cycle, another strategy, increasing the activities of AceA and YcdW, was used to pull the carbon flux to glycolate. Another copy of the *ycdW* gene (with T7 promoter) and *aceA* gene (with PrrnD promoter) were integrated into *araBAD* and *mgsA* sites, respectively, in the chromosome of strain NZ-Gly066. The resulting strain NZ-Gly303 produced 7.2 g/L glycolate and the acetate to glycolate yield was 0.92 mol/mol, which were 48% and 12% higher than the parent strain NZ-Gly066, respectively (Table 2; Fig. 3).

3.5. Production of glycolate by fed-batch fermentation

Fed-batch fermentation of strain NZ-G303 was performed for glycolate production using acetate and glucose double carbon sources (Fig. 4). In this process, sodium acetate and glucose were used as fed solutions, and acetate was used as neutralizer. Using sodium acetate rather than acetic acid as the feed solution, the reason is that the pH would drop down if acetic acid is directly fed into fermentation broth, affecting the cell growth even though adding NaOH to neutralize acetic acid. But, the neutralized product, sodium acetate would be more convenient, including no using the neutralizer NaOH, no effecting to cell growth, as well as no increase in the cost. On the other hand, sodium acetate usually could not be 100% converted into sodium glycolate during the fermentation process, and some acetate would be used for cell synthesis, leading to release free Na^+ and raise pH. To control the pH and make up for the lack of acetate in the fermentor, acetate was used as neutralizer to control the pH at 7.0. Sodium acetate and acetic acid were both included in the calculations of aetate yield.

The initial concentrations of glucose and acetate are 28 and 3.8 g/L respectively. The feeding rate of glucose was adjusted to maintain the concentration of glucose about 10 g/L. Since it was reported that more than 5 g/L acetate inhibited *E. coli* cell growth (Chong et al., 2013; Lee et al., 2016), sodium acetate solution was gradually added into the fermentor to keep the final acetate concentration less than 5 g/L in the fermentor. After 70 h, 73.3 g/L glycolate was produced with a productivity of 1.04 g/(L·h). The acetate to glycolate yield was 0.85 mol/mol (1.08 g/g), while glucose to glycolate yield was 6.1 mol/mol (2.58 g/g). This was the highest reported glycolate titer and yield produced from acetate.

4. Conclusions

To increase carbon yield, a synergetic system for simultaneous utilization of acetate and glucose was designed for production of glycolate in this study. Acetate is the main carbon source to provide carbon backbone while glucose is an auxiliary carbon source to provide NADPH. The glucose metabolic module was engineered through inactivation of phosphofructokinase to generate 6 mol of NADPH from 1 mol of glucose. Through systematic engineering of module I (activation of four enzymes for efficient conversion of acetate to glycolate) and module II (inactivation of Pfk and PTS, as well as activation of PPP, to generate NADPH from glucose), an engineered *E. coli* strain NZ-Gly303 was obtained, which produced 73.3 g/L glycolate with a productivity of 1.04 g/(L·h) in fed-batch fermentation. Moreover, the carbon molar yield was 0.6 mol/mol, which reached 80% of the theoretical maximum. Considering the low price of acetate, this method could obviously reduce the production cost of glycolate.

CRediT authorship contribution statement

Yong Yu: Investigation, Data curation, Writing - review & editing. **Mengyao Shao:** Investigation, Data curation, Writing - review & editing. **Di Li:** Investigation, Data curation. **Feiyu Fan:** Methodology, Software. **Hongtao Xu:** Investigation, Data curation. **Fuping Lu:** Resources. **Changhao Bi:** Resources. **Xinna Zhu:** Conceptualization, Writing - review & editing, Software, Formal analysis, Funding acquisition, Resources, Project administration. **Xueli Zhang:** Conceptualization, Writing - review & editing, Funding acquisition, Resources, Supervision.

Declaration of competing interest

This work has been included in patent application by the Tianjin Institute of Industrial Biotechnology.

Acknowledgments:

This research was supported by grants from National Key R&D Program of China (2018YFA0901400) and the National Natural Science Foundation of China (31870058).

Appendix A. Supplementary data

Supplementary data to this article can be found online at https://doi.org/10.1016/j.ymben.2020.06.001.

Module I: conversion of acetate to glycolate; Module II: reducing equivalent generation pathway. The dotted line means that the pathway is inhibited or inactivated. The symbol Δ represents that the corresponding gene in gray is knocked out. The gene or pathway in gray represents inactivated or inhibited. A gene in red represents activated. The numbers in boxed before metabolites are stoichiometry. Abbreviations: Glu, glucose; Ace, acetate; G6P, glucose-6-phosphate; 6PGL, gluconolactone-6-phosphate; 6PGC, 6-phosphogluconate; RL5P, ribulose-5-phosphate; X5P, xylulose-5-phosphate; R5P, ribose-5-phosphate; S7P, sedoheptulose-7-phosphate; E4P, erythrose-4-phosphate; F6P, fructose-6-phosphate; FBP, fructose-1,6-bisphosphate; G3P, glycerate-3-phosphate; PEP, phosphoenolpyruvate; Pyr: pyruvate; LA, lactate; Ac-CoA, acetyl-CoA; OAA, oxaloacetate; IsoCit, isocitrate; SUC, succinate; MAL, malate; FUM, fumarate; GLYX, glyoxylate, GA, glycolate, TS, tartronate semialdehyde; GLAD, glycolaldehyde; KG, α-ketoglutarate; Suc-CoA, succinyl-CoA; galP, galactose: H+ symporter; glk, glucokinase; ptsI, PTS enzyme I; zwf, glucose-6-phosphate dehydrogenase; pgl, 6-phosphogluconolactonase; gnd, 6-phosphogluconate dehydrogenase; rpe, ribulose-phosphate 3-epimerase; rpiAB, ribose-5-phosphate isomerase A and B; tktA, transketolase 1; tktB, transketolase

2; pfkA, 6-phosphofructokinase 1; pfkB, 6-phosphofructokinase 2; sthA, soluble pyridine nucleotide transhydrogenase; ldhA, D-lactate dehydrogenase; acs, acetyl-CoA synthetase; gltA, citrate synthase; acnA, aconitate hydratase A; aceA, isocitrate lyase; iclR, Isocitrate lyase Regulator; icdA, isocitrate dehydrogenase; sucAB, 2-oxoglutarate decarboxylase and dihydrolipoyltranssuccinylase; lpd, lipoamide dehydrogenase; sucCD, succinyl-CoA synthetase subunit α and β; sdh, succinate dehydrogenase; fum, fumarase; mdh, malate dehydrogenase; ycdW, glyoxylate reductase; gcl, glyoxylate carboligase; aldA, aldehyde dehydrogenase; glcDEF, glycolate dehydrogenase.

References

Bogorad, I.W., Lin, T.S., Liao, J.C., 2013. Synthetic non-oxidative glycolysis enables complete carbon conservation. Nature 502, 693–697.

Castano-Cerezo, S., Pastor, J.M., Renilla, S., Bernal, V., Iborra, J.L., Canovas, M., 2009. An insight into the role of phosphotransacetylase (pta) and the acetate/acetyl-CoA node in *Escherichia coli*. Microb. Cell Fact 8, 54.

Chen, J., Zhu, X., Tan, Z., Xu, H., Tang, J., Xiao, D., Zhang, X., 2014. Activating C4-dicarboxylate transporters DcuB and DcuC for improving succinate production. Appl. Microbiol. Biotechnol. 98, 2197–2205.

Chong, H., Huang, L., Yeow, J., Wang, I., Zhang, H., Song, H.S., 2013. Improving ethanol tolerance of *Escherichia coli* by rewiring its global regulator cAMP receptor protein (CRP). PloS One 8, 1–10.

Dischert, W., Soucaille, P., 2015. Method for Producing High Amount of Glycolic Acid by Fermentation. U. S. Patent US8945888B2.

Deng, Y., Ma, N., Zhu, K., Mao, Y., Wei, X., Zhao, Y., 2018. Balancing the carbon flux distributions between the TCA cycle and glyoxylate shunt to produce glycolate at high yield and titer in *Escherichia coli*. Metab. Eng. 46, 28–34.

Flamholz, A., Noor, E., Bar-Even, A., Milo, R., 2012. eQuilibrator–the biochemical thermodynamics calculator. Nucleic Acids Res. 40, D770–D775.

He, Y.C., Xu, J.H., Su, J.H., Zhou, L., 2010. Bioproduction of glycolic acid from glycolonitrile with a new bacterial isolate of *Alcaligenes* sp. ECU0401. Appl. Biochem. Biotechnol. 160, 1428–1440.

Hinkle, P.C., 1981. Coupling ratios of proton transport by mitochondria. In: Chemiosmotic Proton Circuits in Biological Membranes. Addison-Wesley, Reading, pp. 49–58.

Holms, W.H., Bennett, P.M., 1971. Regulation of isocitrate dehydrogenase activity in *Escherichia coli* on adaptation to acetate. J. Gen. Microbiol. 65, 57–68.

Honer Zu Bentrup, K., Miczak, A., Swenson, D.L., Russell, D.G., 1999. Characterization of activity and expression of isocitrate lyase in *Mycobacterium avium* and *Mycobacterium tuberculosis*. J. Bacteriol. 181, 7161–7167.

Kabir, M.M., Shimizu, K., 2003. Gene expression patterns for metabolic pathway in *pgi* knockout *Escherichia coli* with and without *phb* genes based on RT-PCR. J. Biotechnol. 105, 11–31.

Kataoka, M., Sasaki, M., Hidalgo, A.R., Nakano, M., Shimizu, S., 2001. Glycolic acid production using ethylene glycol-oxidizing microorganisms. Biosc. Biotech. Biochem. 65, 2265–2270.

Kim, S., Lee, C.H., Nam, S.W., Kim, P., 2011. Alteration of reducing powers in an isogenic phosphoglucose isomerase (*pgi*)-disrupted *Escherichia coli* expressing NAD(P)-dependent malic enzymes and NADP-dependent glyceraldehyde 3-phosphate dehydrogenase. Lett. Appl. Microbiol. 52, 433–440.

Koivistoinen, O.M., Kuivanen, J., Barth, D., Turkia, H., Pitkanen, J.P., Penttila, M., Richard, P., 2013. Glycolic acid production in the engineered yeasts *Saccharomyces cerevisiae* and *Kluyveromyces lactis*. Microb. Cell Factories 12, 82.

Lee, H.M., Jeon, B.Y., Oh, M.K., 2016. Microbial production of ethanol from acetate by engineered *Ralstonia eutropha*. Biotechnol. Bioproc. Eng. 21, 402–407.

Lin, P., Jaeger, A.J., Wu, T., Xu, S., Lee, A.S., Gao, F., Chen, P., Liao, J.C., 2018. Construction and evolution of an *Escherichia coli* strain relying on nonoxidative glycolysis for sugar catabolism. Proc. Natl. Acad. Sci. U.S.A. 115, 3538–3546.

Loder, D.J., 1939. Process of Manufacture of Glycolic Acid. E. I. du Pont de Nemours and Company, Wilmington, Del., USA.

Lu, J., Tang, J., Liu, Y., Zhu, X., Zhang, T., Zhang, X., 2012. Combinatorial modulation of *galP* and *glk* gene expression for improved alternative glucose utilization. Appl. Microbiol. Biotechnol. 93, 2455–2462.

Noh, M.H., Lim, H.G., Woo, S.H., Song, J., Jung, G.Y., 2018. Production of itaconic acid from acetate by engineering acid-tolerant *Escherichia coli* W. Biotechnol. Bioeng. 115, 729–738.

Sauer, U., Canonaco, F., Heri, S., Perrenoud, A., Fischer, E., 2004. The soluble and membrane-bound transhydrogenases UdhA and PntAB have divergent functions in NADPH metabolism of *Escherichia coli*. J. Biol. Chem. 279, 6613–6619.

Siedler, S., Lindner, S.N., Bringer, S., Wendisch, V.F., Bott, M., 2013. Reductive whole-cell biotransformation with *Corynebacterium glutamicum*: improvement of NADPH generation from glucose by a cyclized pentose phosphate pathway using *pfkA* and *gapA* deletion mutants. Appl. Microbiol. Biotechnol. 97, 143–152.

Sobota, J.M., Imlay, J.A., 2011. Iron enzyme ribulose-5-phosphate 3-epimerase in *Escherichia coli* is rapidly damaged by hydrogen peroxide but can be protected by manganese. Proc. Natl. Acad. Sci. U. S. A. 108, 5402–5407.

Stanford, D.R., Whitney, M.L., Hurto, R.L., Eisaman, D.M., Shen, W.C., Hopper, A.K., 2004. Division of labor among the yeast Sol proteins implicated in tRNA nuclear export and carbohydrate metabolism. Genetics 168, 117–127.

Tan, Z., Zhu, X., Chen, J., Li, Q., Zhang, X., 2013. Activating phosphoenolpyruvate carboxylase and phosphoenolpyruvate carboxykinase in combination for improvement of succinate production. Appl. Environ. Microbiol. 79, 4838–4844.

Tan, Z., Chen, J., Zhang, X., 2016. Systematic engineering of pentose phosphate pathway improves *Escherichia coli* succinate production. Biotechnol. Biofuels 9, 262.

Temme, K., Hill, R., Segall-Shapiro, T.H., Moser, F., Voigt, C.A., 2012. Modular control of multiple pathways using engineered orthogonal T7 polymerases. Nucleic Acids Res. 40, 8773–8781.

Underwood, S.A., Buszko, M.L., Shanmugam, K.T., Ingram, L.O., 2002. Flux through citrate synthase limits the growth of ethanologenic *Escherichia coli* KO11 during xylose fermentation. Appl. Environ. Microbiol. 68, 1071–1081.

Walsh, K., Koshland, D., 1985. Characterization of rate-controlling steps in vivo by use of an adjustable vector. Proc. Natl. Acad. Sci. U.S.A. 82, 3577–3581.

Wang, Y., San, K.Y., Bennett, G.N., 2013. Improvement of NADPH bioavailability in *Escherichia coli* through the use of phosphofructokinase deficient strains. Appl. Microbiol. Biotechnol. 97, 6883–6893.

Wei, G., Yang, X., Gan, T., Zhou, W., Lin, J., Wei, D., 2009. High cell density fermentation of *Gluconobacter oxydans* DSM 2003 for glycolic acid production. J. Ind. Microbiol. Biotechnol. 36, 1029–1034.

Xiao, Y., Ruan, Z., Liu, Z., Wu, S., Varman, A.M., Liu, Y., Tang, Y., 2013. Engineering *Escherichia coli* to convert acetic acid to free fatty acids. Biochem. Eng. J. 76, 60–69.

Zahoor, A., Otten, A., Wendisch, V.F., 2014. Metabolic engineering of *Corynebacterium glutamicum* for glycolate production. J. Biotechnol. 192 Pt B, 366–375.

Zhao, J., Li, Q., Sun, T., Zhu, X., Xu, H., Tang, J., Zhang, X., Ma, Y., 2013. Engineering central metabolic modules of *Escherichia coli* for improving beta-carotene production. Metab. Eng. 17, 42–50.

Zhao, D., Yuan, S., Xiong, B., Sun, H., Ye, L., Li, J., Zhang, X., Bi, C., 2016. Development of a fast and easy method for *Escherichia coli* genome editing with CRISPR/Cas9. Microb. Cell Factories 15, 205.

Zheng, J., Jia, Z., 2010. Structure of the bifunctional isocitrate dehydrogenase kinase/phosphatase. Nature 465, 961–965.

Zhu, K., Li, G., Wei, R., Mao, Y., Zhao, Y., He, A., Bai, Z., Deng, Y., 2019. Systematic analysis of the effects of different nitrogen source and ICDH knockout on glycolate synthesis in *Escherichia coli*. J. Biol. Eng. 13, 30.

Zhu, X., Tan, Z., Xu, H., Chen, J., Tang, J., Zhang, X., 2014. Metabolic evolution of two reducing equivalent-conserving pathways for high-yield succinate production in *Escherichia coli*. Metab. Eng. 24, 87–96.

Zhu, X.N., Zhao, D.D., Qiu, H.N., Fan, F.Y., Man, S.L., Bi, C.H., Zhang, X.L., 2017. The CRISPR/Cas9-facilitated multiplex pathway optimization (CFPO) technique and its application to improve the *Escherichia coli* xylose utilization pathway. Metab. Eng. 43, 37–45.